Available online at www.sciencedirect.com
SCIENCE DIRECT®
Polymer 45 (2004) 409–421
polymer
www.elsevier.com/locate/polymer

Ultradrawing of blend films of ethylene-dimethyl-aminoethyl methacrylate copolymer and ultra-high molecular weight polyethylene prepared by gelation/crystallization from solutions

Mami Azuma[a], Lin Ma[a], Chunqing He[b], Takenori Suzuki[b], Yuezhen Bin[a], Hiromichi Kurosu[a], Masaru Matsuo[a,*]

[a]*Textile and Apparel Science, Faculty of Human Life and Environment, Nara Women's University, Nara 630-8263, Japan*
[b]*Radiation Science Center of High Energy Accelerator Research Organization, 1-1 Oho, Tsukuba, Ibaraki 305-0801, Japan*

Received 21 February 2003; received in revised form 11 September 2003; accepted 12 September 2003

Abstract

Copolymer ethylene-dimethyl-aminoethyl methacrylate (EDAM) with 3.9% DAM side groups and ultra-high molecular weight polyethylene (UHMWPE) were blended in decalin solvent. The hot homogenized solution was poured into an aluminum tray to form gels and the decalin was allowed to evaporate from the resultant gels under ambient condition. Surprisingly, the resultant dry blend films could be elongated to more than 200-fold ($\lambda = 200$) even for the blend film with 90% EDAM content (9/1 composition), although the maximum draw ratio of EDAM homopolymer films was 1.6-fold ($\lambda = 1.6$). The mechanism of the great drawability was dependent upon the content of EDAM. The drawability for the 9/1 composite films was attributed to large crystal lamellae of UHMWPE ensuring crystal transition from a folded to a fibrous type. Accordingly, EDAM chains were independent of ultradrawing of UHMWPE and kept a random orientation under ultra-drawing process. The storage (Young's) modulus was 10 GPa at 20 °C. In contrast, EDAM chains within the 1/1 composite films were oriented drastically together with UHMWPE crystallites. The modulus of the 1/1 composition at 20 °C reached 68 GPa, which was higher than the value (40 GPa) of polypropylene films with $\lambda = 100$. Such considerable difference of modulus due to EDAM content was analyzed in relation to the gelation/crystallization from solutions.

Keywords: Copolymer ethylene-dimethyl-aminoethyl methacrylate (EDAM); Ultra-high molecular weight polyethylene (UHMWPE); Dry blend films

1. Introduction

In the previous papers [1,2], effect of side groups on the crystallization of ethylene main chains was investigated by using copolymer ethylene-methyl methacrylate (EMMA) and copolymer ethylene-dimethyl-aminoethyl methacrylate (EDAM). The result revealed the longer ethylene sequences in the non-crystalline phase had a non-random local arrangement but the bulky volume of the MMA side groups suppresses crystallization of ethylene sequences. Consequently, even though crystallization is suppressed, the tendency for longer ethylene sequences to self-order leads to a dynamic local ordering in the non-crystalline phase. Furthermore, the EMMA films drawn up to their maximum draw ratio caused the drastic shrinkage, as well as drastic stress-relaxation by chain slippage under a constant strain at room temperature.

This paper deals with the characteristics of copolymer EDAM and the blends with ultra-high molecular weight polyethylene (UHMWPE). The preparation of the blend films is based on the improvements of mechanical properties and the dimensional stability of EDAM films. Because ultra-drawn polyethylene fibers and films exhibit excellent mechanical properties with Young's modulus of 100–220 GPa and tensile strength of 3–6 GPa as well as excellent dimensional stability at elevated temperature close to the melting point [3–7]. However, the poor dyeing property and poor lamination of polyethylene films are big problems to expand the utility in commercial level. Blending polyethylene with other polymers having polar groups is one of the possible strategies in overcoming this problem. Unfortunately, no successful representation of

* Corresponding author. Fax: +81-742-20-3462.
E-mail address: m-matsuo@cc.nara-un.ac.jp (M. Matsuo).

0032-3861/$ - see front matter © 2003 Elsevier Ltd. All rights reserved.
doi:10.1016/j.polymer.2003.09.031

high modulus and high strength fibers and/or films has been achieved for the blends of UHMWPE and other polymers except the polyethylene/polypropylene blend system [8,9].

The main purpose is concentrated on the relation of morphology and mechanical properties of ultra-drawn blend films of UHMWPE and EDAM having polar groups by gelation/crystallization from solutions. To assure dimensional stability of the drawn EDAM films, how to get stable crystallization of the ethylene sequences of EDAM is one of the important factors. As one of trials, EDAM and UHMWPE blends are prepared by gelation/crystallization from dilute solutions in this paper. Surprisingly, the elongation of the dry blend films with 90% EDAM reached to 200 folds ($\lambda = 200$), while the maximum draw ratio of the 1/1 composition was 500-folds. For the ultra-drawn blend films with the 9/1 and 1/1 compositions, no shrinkage occurred at room temperature for the drawn blends. The greatest drawability and excellent thermal dimensional stability are investigated by using DSC, X-ray, ^{13}C NMR, and positron-annihilation in the viewpoint of co-crystallization of ethylene sequences between EDAM and UHMWPE.

2. Experimental section

The materials used in the present work were EDAM and UHMWPE. Two EDAM samples, EDAM-I and EDAM-II with different contents of DAM, were furnished by Sumitomo Chemical Co. Ltd. UHMWPE (Hervules 1900/90189) has a molecular weight of 6×10^6. The structural characteristics of EDAM-I, EDAM-II and UHMWPE are listed in Table 1. In preparing the blend samples, the concentration of UHMWPE was fixed to be 0.4 g/100 ml against solvent. The amount of EDAM was determined relative to that of the UHMWPE and 0.4 g/100 ml was the optimum concentration of the UHMWPE solutions to prepare high modulus and high strength films [7]. The compositions of EDAM and UHMWPE chosen were 9/1 and 1/1. Solvent was decalin.

The solution was prepared by heating the well-blended polymer/solvent mixture at 135 °C for 40 min under nitrogen. The homogenized solution was quenched to room temperature by pouring it into an aluminum tray, thus generating a gel. The decalin was allowed to evaporate from the gels under ambient conditions. The resulting dry gel film was vacuum-dried for one day to remove any residual trace of decalin, and then elongated manually up to desired draw ratios at 135 °C under nitrogen.

In the preliminary experiments, the solvent cast films of EDAM-I and EDAM-II homo-polymers were prepared, since the EDAM cannot form gels by quenching solution to room temperature. All the characteristics of the resultant films were confirmed to be perfectly equal to those of their melt described in the previous paper [1].

2.1. Small angle light scattering

Small angle light scattering (SALS) patterns (Hv patterns) under polarization condition were obtained with a 3-mW He–Ne gas laser as a light source. Diffuse scattering was avoided by sandwiching the specimen between cover glasses with silicon oil as an immersion fluid.

Table 1
Characterization of EDAM and UHMWPE films

Specimen		DAM (mol%)	Melting point (°C)	Draw ratio (maximum)	Molecular weight	
					$M_n(10^4)$	$M_w(10^4)$
EDAM-I (DA3023)	Annealed	3.9	97	1.6	2.43	8.88
	Quenched			1.6		
EDAM-II (DA3031)	Annealed	4.1	66	1.6	2.93	8.29
	Quenched			3.0		
UHMWPE			142	300	6×10^6	

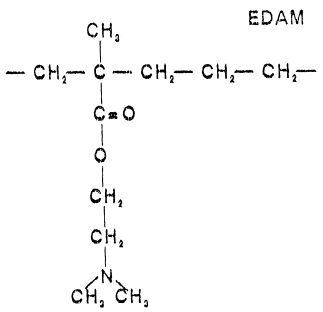

2.2. X-ray

The X-ray measurements were carried out with a 12 kW rotating-anode X-ray generator (Rigaku RAD-rA). The X-ray beam by Cu K_α radiation at 200 mA and 40 kV was monochromatized with a curved graphite monochromater. WAXD intensity distribution was obtained at desired temperatures from −130 to 135 °C by using a curved position sensitive proportional counter (PSPC). To pursue the exact measurement of the diffraction intensity, the accumulated time was set to be 10 min at each temperature.

2.3. ^{13}C NMR

NMR measurements as a function of temperature were carried out for the EDAM melt films on a JEOL, JM-EX 270 spectrometer, operating at 67.8 MHz for ^{13}C. The measurements were done at room temperature. The actual temperatures in the probe under spinning were confirmed to be in the range of 27–36 °C. The magic-angle spinning rate was 5–5.5 kHz. The contact time in ^{13}C CP/MAS measurement was 2 ms. The chemical shifts were determined relative to the higher field signal (29.5 ppm) of adamantane.

2.4. Positron-annihilation

The positron-annihilation experiments were conducted with a conventional fast–fast coincidence system having a time resolution of 300 ps full width at half maximum (FWHM) [2]. The time spectrometer was composed of two plastic scintillation detectors (40 mm ∅ × 40 mm Pilot-U mounted on a Hamamatsu H1949 photomultiplier), two differential constant fraction discriminators (ORTEC 583) (one for start signals from 1.28 MeV γ-rays and the other one for stop signals from 0.511 MeV annihilation γ-rays), a time-to-amplitude converter (ORTEC 4570), and a multi-channel analyzer with a 1024 conversion gain (SEIKO 7800). The accumulated data was controlled by a personal computer (NEC-PC).

A position source was prepared by depositing ca 1.1 MBq (30 μ Ci) of aqueous $^{22}NaCl$ on a Kapton foil of 7 μm thickness and 10 × 10 mm^2 area. After drying, the foil was covered with the same size of foil and the edges were glued with epoxy resin. The source was further sealed in a 3 μm Mylar foil, and then sandwiched by two identical samples for positron-annihilation measurements. The diameter of the spot of the ^{22}Na source was ca 2 mm ∅.

During the measurement, samples were kept in a vacuum cell, in which the temperature of samples was controlled. Spectra were recorded every hour and about 1–2 million events were stored in each spectrum. Thus, a positron-annihilation spectrum with high statistics was obtained, and the ortho-positronium (*o*-Ps) component became resolvable into two components.

2.5. Visco-elastic measurements

The complex dynamic tensile modulus was measured at 10 Hz over the temperature range from −150 to 150 °C by using a visco-elastic spectrometer (VES-F) obtained from Iwamoto Machine Co. Ltd. The length of the specimen between the jaws was 40 mm and the width was about 1.5 mm. The complex dynamic modulus was measured by imposing a small dynamic strain to ensure linear visco-elastic behavior of the specimen [10]. In doing so, the specimen was subjected to a static tensile strain in the range of 0.05–0.1%, in order to place the sample in tension during the axial sinusoidal oscillation.

2.6. DSC measurements

The calorimetric investigations of EDAM and their blends were performed with an Exstar 6100 of Seiko Instrument Incorporation. The heating rate was 1 °C/mm. The weight of specimen was 10 mg. The crystallinity was computed from DSC curves by assuming the heat of fusion at equilibrium melting temperature of fully crystalline of PE to be 286.8 J/g.

3. Results and discussion

Before starting the discussion for the characteristics of EDAM/UHMWPE blend films, we shall describe the characteristics of EDAM prepared from dilute solution. For EDAM-I, Hv light scattering pattern showed a four-leaf clover type, indicating scattering from perfect spherulites with the maximum intensity at odd multiples of the azimuthal angle (μ) of 45° and with zero intensity at the scattering center ($\theta = 0°$). The average radius of spherulites was 4.68 μm as has been reported for the melt film [1]. When the specimen was elongated to $\lambda = 1.6$, the lobes were extended in the horizontal direction. This deviates from deformation of perfect spherulites associated with the change from a sphere to an ellipsoid while keeping uniform deformation with respect to the radial direction and/or large optical density fluctuation within the spherulite. Such changing mode is perfectly equal to that for the melt films discussed in the previous paper (see Fig. 3 in Ref. [1]. The specimen kept at $\lambda = 1.6$ was cut within 30 min. Such disruption was probably thought to be due to the molecular slippage by disentanglement of oriented EDAM-I chains.

As for EDAM-II specimen, the Hv scattering from spherulites with the average radius of 2.94 μm was observed. When EDAM-II specimen was stretched up to the maximum draw ratio ($\lambda = 3.0$), the scattering shows the superposition of broad four-leaf lobes and sharp streaks as shown in Fig. 1. The streaks are surely attributed to the fissures parallel to the stretching direction, which were observed under polarized light microscopy. As discussed in the previous paper [1], silicon oil with a refractive index similar to the refractive index of the specimen was spread on the surface of the specimen at a fixed state. Actually, as shown in Fig. 1, the streaks were not observed for the specimen after 48 h but observed within 3 h, because of insufficient immersion of the silicon oil into the fissures

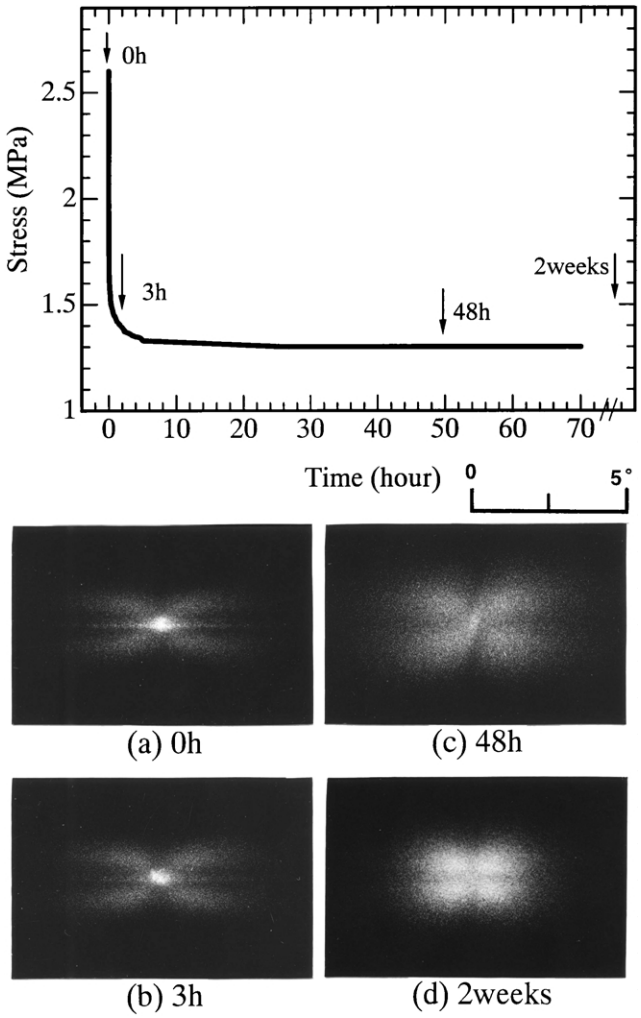

Fig. 1. Time-dependence of stress relaxation for the EDAM-II quenched film with $\lambda = 3$ and the Hv patterns observed at the indicated times.

within the specimen. The drastic stress relaxation is due to molecular slippage by disentanglements. This causes more promotion of the scattered intensity by the decrease in orientational disorder of the optical axes with respect to the radial direction. The drastic decrease of the stress within 3 h at a fixed state caused the drastic shrinkage of the specimen, when the elongated specimen was removed from the stretcher. To improve poor dimensional stability and poor drawability of EDAM specimens, EDAM and UHMWPE blends were prepared by gelation/crystallization from dilute solution and elongated. In the following experiments, EDAM-I was used as a test specimen. Because, EDAM-I shows such a typical mechanical behavior that the maximum elongation was 1.6 and the film kept at the same draw ratio was cut within 30 min indicating drastic molecular slippage by disentanglements. Furthermore, drastic shrinkage occurred when the specimen drawn up to $\lambda = 1.6$ removed from the stretcher and this tendency is more considerable than the behavior of EDAM-II.

Fig. 2 shows DSC curves for EDAM and UHMWPE blend gels containing solvent, in which the concentration of

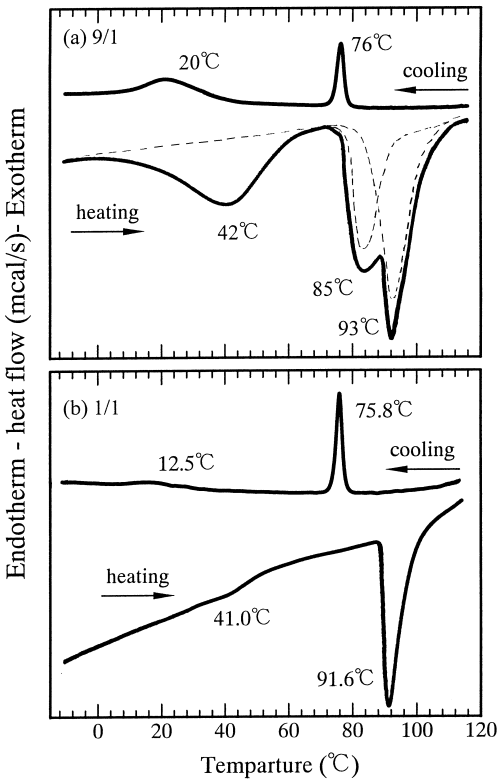

Fig. 2. DSC curves in the heating and cooing process for EDAM-I and UHMWPE blend gels at the indicated composition.

UHMWPE was found to be 0.4 g/100 ml against decalin solvent described in Section 2. The curves were obtained by quenching the mixed solution from 135 to −10 °C and then by heating the resultant gel from −10 to 135 °C, in which decalin was adopted as reference. It is obvious that the exotherm peak appeared at lower temperature <20 °C is associated with the crystallization of the ethylene sequence of EDAM under cooling process of solutions, while the corresponding endotherm peak at lower temperature <42 °C is associated with the melting of the crystallites. In Fig. 2, the exotherm peak at 20 °C and the endotherm peak at 42 °C for the 9/1 composite gel show clear profiles. In contrast, the exotherm peak of the solution with 1/1 composition (50% EDAM-I content) appeared at 12.5 °C is much smaller than that with 9/1 composition (90% EDAM-I content) appeared at 20 °C. The same tendency is also observed for endotherm peak under the heating process. This suggests that most of EDAM-I chains are co-crystallized with UHMWPE chains within the 1/1 composite gel and very few crystallites exist independently apart from the co-crystallites, which indicates that the crystallization mode of ethylene sequence of EDAM-I is strongly dependent upon EDAM content within the blend. The detailed analysis revealed that in the temperature range >75 °C, the exotherm peak area of the 9/1 composite gel is about 1/2 for that of the 1/1 composition and the peak position appears at higher temperature side, although the amount of UHMWPE within the 9/1 composite gel is 20% in

Table 2
The long period of EDAM-I/UHMWPE blend films with different compositions

EDAM-I/UHMWPE	0/1	1/1	9/1	1/0
L (Å)	111.5	110.1	101.4	91.2

comparison with that within the 1/1 composite gel. Accordingly, the peaks of the 9/1 composition are thought to be due to the melting of stable UHMWPE crystallites in gels, while the peaks of the 1/1 composition are thought to be due to the melting of crystallites formed by the co-crystallization of UHMWPE and EDAM-I, indicating that the co-crystallites are slightly less stable than UHMWPE homopolymer crystallites.

The endotherm peak of the 9/1 gel at higher temperature side shows two peaks at 85 and 93 °C, respectively. Judging from the content of EDAM, the peak at 85 °C is thought to be due to the melting of EDAM crystallites with large size, while the peak at 42 °C, the melting of the small size EDAM crystallites. The peak at 93 °C for the 9/1 blend gel is obviously attributed to the melting of UHMWPE crystallites, while that of 91.6 °C for the 1/1 blend is obviously attributed to the melting of co-crystallites of EDAM and UHMWPE. As discussed for the exotherm peak at higher temperature, the comparison of melting temperature of the co-crystallites between thee 9/1 and 1/1 blend gels indicates that the co-crystallites of EDAM and UHMWPE are slightly less stable and smaller than UHMWPE crystallites. The co-crystallization for the 1/1 blend can be justified from the result that the peak of EDAM at 41 °C is much smaller than that at 42 °C for the 9/1 blend, although the EDAM content within the 1/1 blend is about 20% in comparison with the content within the 9/1 blend.

Fig. 3 shows WAXD patterns observed from undrawn blend films prepared by evaporating solvents. X-ray beam was directed parallel to the film surface. The characteristic diffractions from the (110) and the (200) planes for the composite films indicate the preferential orientation of the c-axis perpendicular to the film surface, which is similar to the diffraction intensity from single crystal mats. This tendency becomes clearer as the EDAM content decreases. On the other hand, the diffraction rings for the pattern of the EDAM film indicate a random orientation of crystallites.

Fig. 4 shows SAXS intensity distributions (end view) of the undrawn blend films and the individual homo-polymer (EDAM-I and UHMWPE) films as a function of scattering angle $2\theta_B$ in the meridional direction by PSPC system. The intensity distribution from the blend films shows scattering maxima corresponding to long periods. The values are listed in Table 2. With increasing the EDAM-I contents, the long period becomes shorter. As shown in this figure, the

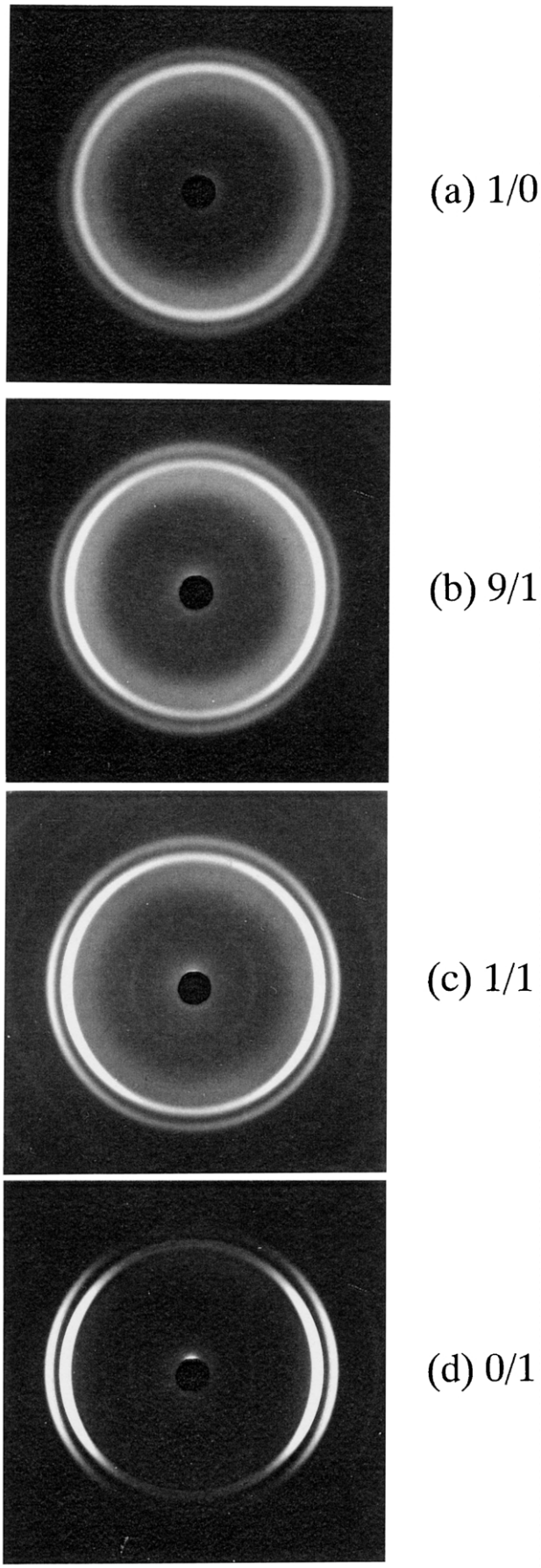

Fig. 3. WAXD patterns (end view) for EDAM-I/UHMWPE blend films with $\lambda = 1$.

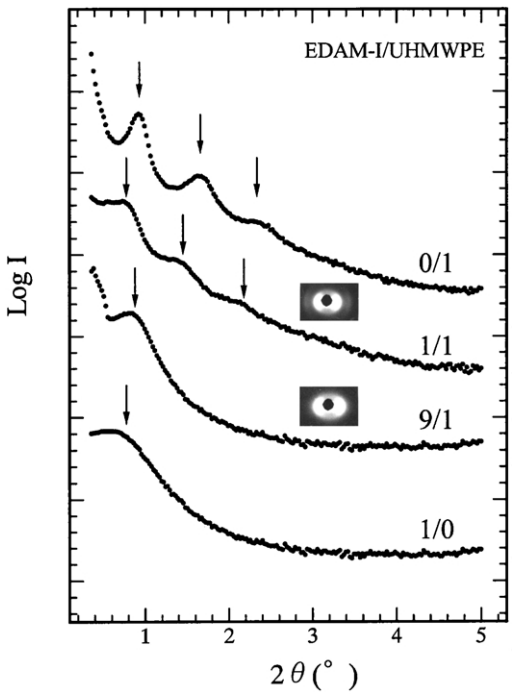

Fig. 4. SAXS intensity distributions for EDAM-I and UHMWPE blend films in the meridional direction.

scattering maxima become less distinct as EDAM content increases. The SAXS distributions and WAXD patterns together indicate that the 1/1 blend is composed of highly oriented crystal lamellae with their flat face parallel to the film surface like UHMWPE (0/1), but the orientation fluctuation of crystal lamellae become more pronounced with increasing EDAM content. The profile of the intensity distribution from the EDAM (1/0) shows a monotonous curve with an indistinct small peak. Here, it may be expected that the isolated UHMWPE chains within the 9/1 composite film also form large crystal lamellae of UHMWPE under the gelation but the crystal lamellae cannot orient parallel to the film surface. This is thought to be due to the fact that large amounts of EDAM hamper the ordered orientation of the lamellae of UHMWPE.

Fig. 5 shows WAXD patterns for EDAM/UHMWPE (the 9/1 and 1/1 compositions) blend films drawn up to their maximum ratios. The profiles of WAXD were confirmed to be almost the same for the specimens with $\lambda > 100$. The pattern of the 9/1 composition indicates different orientation modes between EDAM-I and UHMWPE crystallites. That is, the weak diffraction rings from the (110) and (200) planes at $\lambda > 50$ are the reflection from EDAM crystallites with a random orientation, while the sharp diffraction spots are due to the orientation of UHMWPE crystallites with almost perfect orientation with respect to the stretching direction. Beyond 50-folds, the EDAM crystallites tend to orient to the stretching direction. Especially, the pattern of the 1/1 composition shows sharp diffraction spots from the (110) and (200) planes and any ring does not appear, indicating that EDAM-I and UHMWPE crystallites are oriented together in the stretching direction predominantly. Such different orientation modes are attributed to their different crystallization modes under gelation process shown in Fig. 1; co-crystallization of EDAM-I and UHMWPE chains within the 1/1 composite film and separate crystallization of EDAM-I and UHMWPE chains within the 9/1 composite film under gelation process.

Fig. 6 shows WAXD intensity distribution of the 9/1 and 1/1 composite film for EDAM-I and UHMWPE with $\lambda = 100$. The film thickness of the two blends were almost the same. The measurements were done by a special attachment set in the X-ray instrument. The drawn specimen was rotated 60 times/min around a film normal direction. The scanning speed of a detector of diffraction beam was 16 min for 1° (twice the Bragg angle). This method has an advantage to know the approximate average intensity of the diffraction intensity for the drawn films. It is seen that the crystallinity of the 1/1 composite film is much higher than that of the 9/1. Namely, a very broad peak around 18.2° for the 9/1 composite film is due to the contribution from the amorphous phase. The peak profile was similar to the profile observed for an undrawn EDAM-I homopolymer film already (see Fig. 7(c) in Ref. [1]).

To pursue more quantitative analysis, temperature dependence of the diffraction intensity was measured in the range from − 130 to 135 °C. Fig. 7 shows the results for EDAM-I and UHMWPE blends with $\lambda = 100$ and the corresponding UHMWPE homo-polymer. All the specimens were maintained for 10 min at the indicated temperatures before measurements. The measurements were carried out in the horizontal direction, since the special instrument used in Fig. 6 could not be used for the measurements at elevated temperature. In this case, for the 9/1 blend, no peak appears around 18.2° for the 9/1 composition (see Fig. 6). Two peaks correspond to the reflections from the (110) and (200) planes of orthorhombic crystals of EDAM-I and UHMWPE. The large peak shift of the (200) plane to lower angle with increasing temperature is due to the thermal expansion of the *a*-axis. This tendency is most considerable for the 9/1 blend indicating that the diffraction peaks are contributed from unstable state of EDAM-I crystallites. The peaks become less intense with increasing temperature indicating the partial melt of EDAM-I crystallites. In contrast, for the 1/1 composition, the peak intensity is almost independent of temperature. This tendency is slightly similar to temperature dependence of UHMWPE homo-polymer indicating that co-crystallites of EDAM-I and UHMWPE chains within the 1/1 composite film are stable like UHMWPE crystallites. Such considerable different temperature dependence caused by different EDAM contents is due to the fact that the crystallization mode of the ethylene sequences is sensitive to EDAM content within the blend. Namely, the EDAM-I and UHMWPE co-crystallites within the 1/1 composite film are oriented together in the stretching direction and

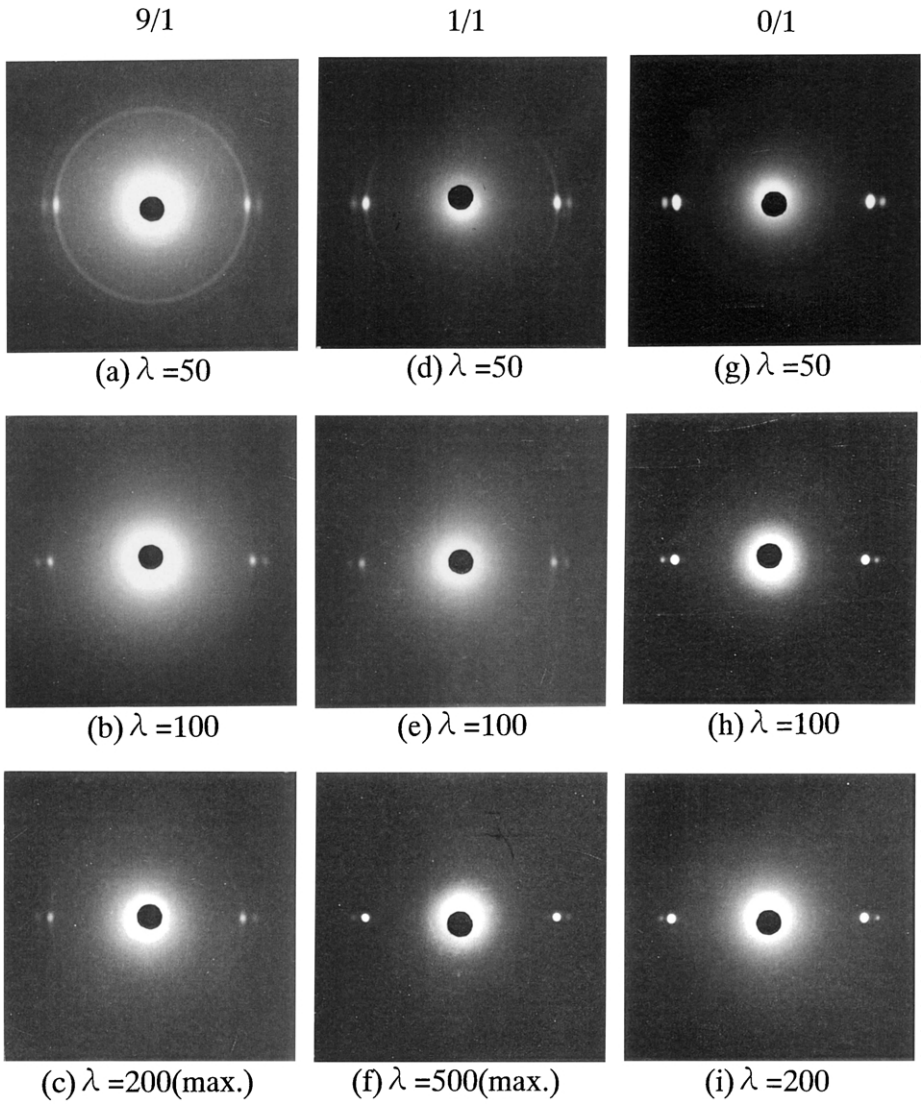

Fig. 5. WAXD patterns (through view) for EDAM-I/UHMWPE blend films at the indicated draw ratios.

consequently melting point of EDAM crystallites is almost equal to that of UHMWPE crystallites. In contrast, EDAM crystallites within the 9/1 composite film take a random orientation and the melting point of EDAM crystallites was close to that of EDAM homopolymer crystallites prepared by melting press [1]. To analyze the different crystallization modes, DSC measurements were done for the 9/1 and 1/1 composition films.

Fig. 8(a) shows the DSC curves for dry blend gel films at $\lambda = 1$ and 100. Fig. 8(b) shows the DSC curves of UHMWPE dry gel films with $\lambda = 1$ and 100 as well as the EDAM-I film with $\lambda = 1$. Two endothermic peaks appear clearly for all 9/1 composite films at temperatures $< 90\,^{\circ}C$ and the 1/1 composite films at temperatures $< 69\,^{\circ}C$ indicating the existence of very small EDAM crystallites. Judging from the endothermic curves of homopolymers, i.e. EDAM-I and UHMWPE in Fig. 8(b), it is evident that the peaks are related to the progression of separate crystallization of EDAM-I and UHMWPE chains under drying and elongation processes. As for the EDAM/UHMWPE blends, the existence of the three peaks indicates the separate crystallization of EDAM-I. Especially at $\lambda = 100$ the clear peak for the 9/1 composition appears at temperatures lower than the peak for UHMWPE. This indicates the suppression of oriented crystallization by large amounts of EDAM chains. For the 1/1 composition, the small peak appears at 69 °C at $\lambda = 1$ indicating separate crystallization of EDAM chains. This justifies the crystallization under gelation observed as very small peak at 12.5 °C in Fig. 2. At $\lambda = 100$, the peak at 69 °C observed for the undrawn film disappears and only a large peak appears at 142 °C, indicating the co-crystallization of EDAM and UHMWPE chains under elongation. If further co-crystallization of EDAM and UHMWPE chains did not occur, the large peak appeared at the same temperature (146 °C) for the UHMWPE film, reflecting only the melting of UHMWPE crystallites. Actually, the crystallinities estimated from the endotherm peaks were 66.2 and 90.7% for

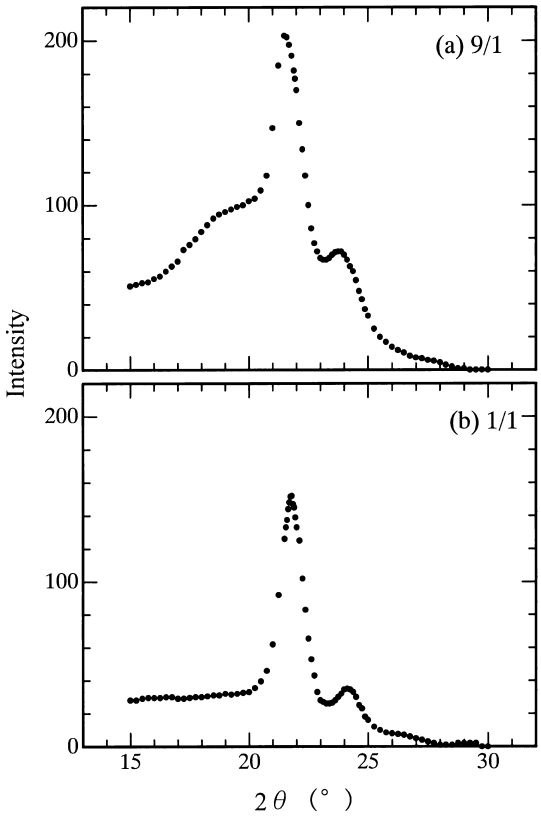

Fig. 6. WAXD intensity distributions of the 9/1 and 1/1 compositions of EDAM-I/UHMWPE blend film with $\lambda = 100$. Specimens were rotated 60 times/min around a film normal direction.

the 1/1 blend gel and UHMWPE gel, respectively at $\lambda = 100$. This also means that the crystallization of EDAM and UHMWPE chains provides small crystallites with a number of defects under gelation/crystallization and elongation processes.

Fig. 9 shows the 67.8 MHz CP (cross polarization)/MAS ^{13}CNMR spectra of the 9/1 and 1/1 composite films (EDAM-I/UHMWPE) with $\lambda = 1$ and 100 at room

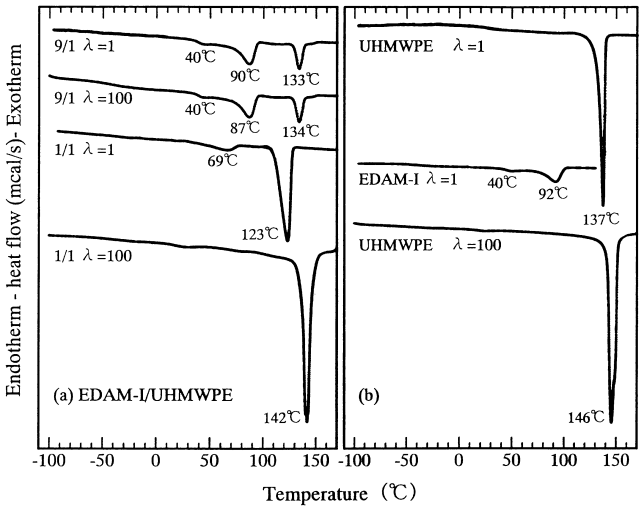

Fig. 8. DSC curves for (a) EDAM-I/UHMWPE (b) UHMWPE, EDAM-I dry gel films at the indicated draw ratios.

temperature. As described in the previous paper [1], the CP/MAS spectra show two peaks with chemical shifts of 32.8 ppm (peak I) and 30.8 ppm (peak II), which can be assigned to the orthorhombic crystalline and non-crystalline methylene carbons in the ethylene sequence, respectively. The assignment of the other peaks was made according to the DD/MAS spectra of EDAM reported already as well as the solution NMR spectra [11]. All the spectra are analyzed on the basis of the assumption of a superposition curve of Gaussian and Lorentzian functions. In this process, the line width and the peak height of each component were determined to give the best fit by computer on the basis of small changes from the initial peak position. The initial values of the all components were given by adopting the corresponding chemical shifts of EDAM and UHMWPE obtained elsewhere [11,12]. The spectrum indicates the existence of the orthorhombic crystal (O), monoclinic crystal (M) and rubbery (R) components [13–15]. As shown in this figure, existence of interfacial component can

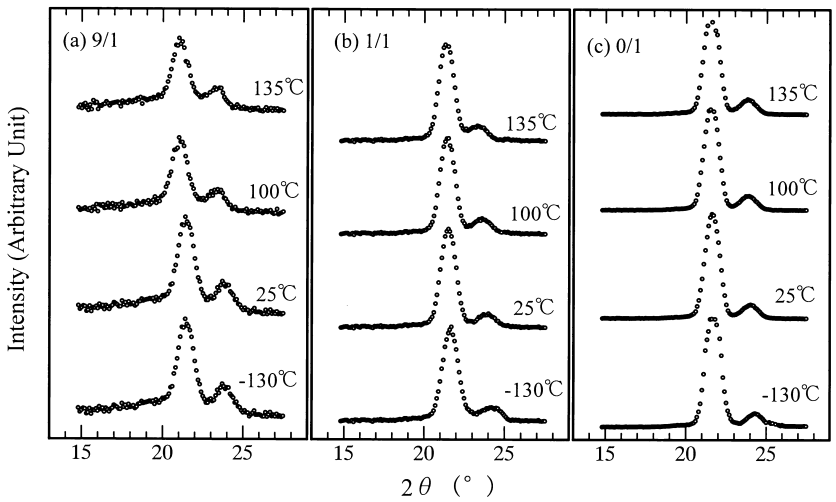

Fig. 7. WAXD intensity distributions for EDAM-I/UHMWPE blend gel films which were drawn to 100 times at elevated temperatures.

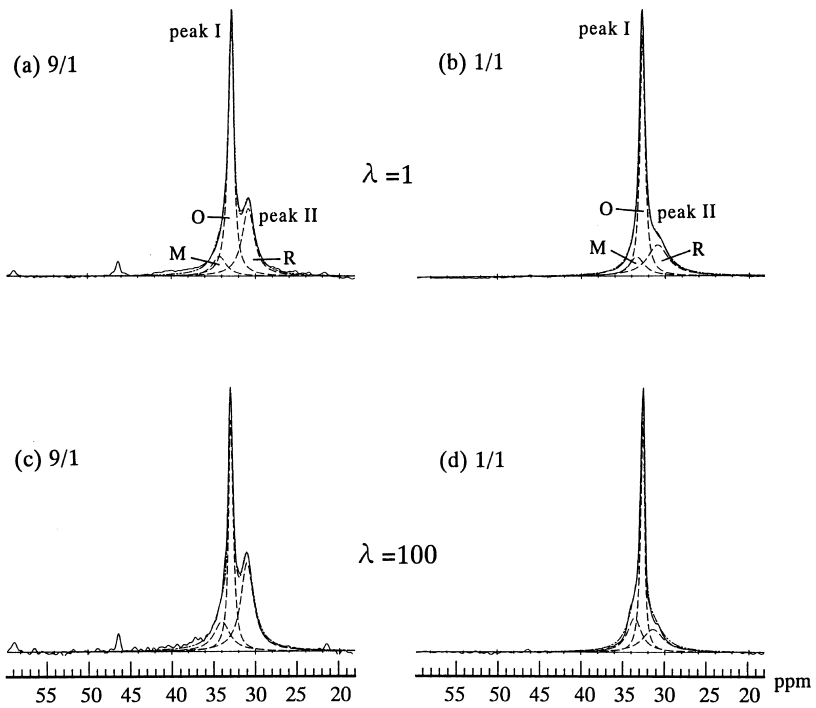

Fig. 9. 67.8 MHz ^{13}C CP/MAS spectra measured for the 9/1 and 1/1 blends at $\lambda = 1$ and 100.

not be observed for the blend films in spite of the appearance for EDAM-I homopolymer [1]. As shown for semi-crystalline polymers, CP/MAS spectra emphasize the contribution of the crystalline phase. Judging from the ^{13}C NMR CP/MAS spectrum of EDAM-I homo-polymer with $\lambda = 1$ [11], the peak I of CP/MAS spectrum of the 9/1 composition with $\lambda = 1$ is attributed mostly to the orthorhombic crystalline signal (O) of UHMWPE, while the peak II, the rubbery signal (R) of non-crystalline phase. Here, the CP/MAS spectra provide almost same profiles of the peak I and peak II for the 9/1 compositions with $\lambda = 1$ and 100. This indicates that elongation up to $\lambda = 100$ causes no significant effect on the local ordering and the oriented crystallization of ethylene sequences in the EDAM amorphous region by elongation. This result is in good agreement with the WAXD patterns in Fig. 5. On the other hand, the peak II of CP/MAS spectrum for the 1/1 composition decreases for the drawn films, indicating a slight increase in crystallinity by oriented crystallization.

Fig. 10 shows changes in strain as a function of time for the 9/1 and 1/1 composite films (EDAM/UHMWPE) with $\lambda = 100$, when a constant stress of 20 MPa is applied as an external excitation. This experiment was carried out to support a series of experimental results by X-ray, DSC, and ^{13}C NMR. It is seen that the strain for the 9/1 composite film increases with time, while a very small increase in strain is observed for the 1/1. This means that partly oriented EDAM chains within the 9/1 composition cause drastic molecular slippage because of very few entanglements between EDAM-I and UHMWPE amorphous chain segments, while EDAM chains with very highly orientation within 1/1 composition are maintained without the slippage by disentanglements indicating the progressive co-crystallization under elongation.

Fig. 11 shows temperature dependence of the storage modulus (E') and the loss modulus (E'') of EDAM/UHMWPE blends at a frequency of 10 Hz measured for the 9/1 and 1/1 composite films of EDAM/UHMWPE as well as UHMWPE homopolymer (0/1) films with $\lambda = 1$ and 100, in addition to the EDAM homopolymer film ($\lambda = 1$). The 1/1 composition with $\lambda = 100$ provides large values of E' beyond 68 GPa at 20 °C, which are lower than the value (100 GPa) of E' for the corresponding UHMWPE but higher than the value (40 GPa) of ultradrawn polypropylene ($\lambda = 100$) [17,18]. In contrast, the values of E' of the 9/1 compositions with $\lambda = 100$ are about 10 GPa, which is

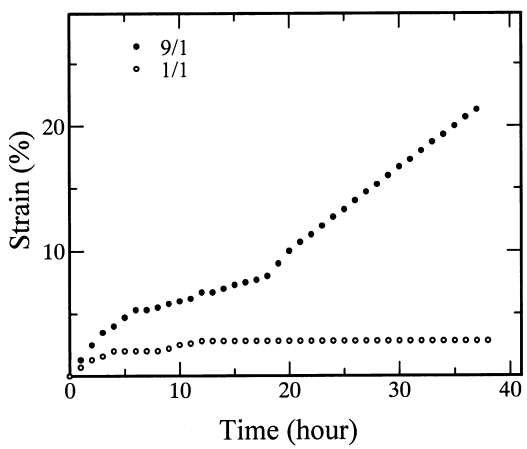

Fig. 10. Changes in strain against time for EDAM-I/UHMWPE blends (9/1,1/1) with $\lambda = 100$ under a constant stress of 20 MPa.

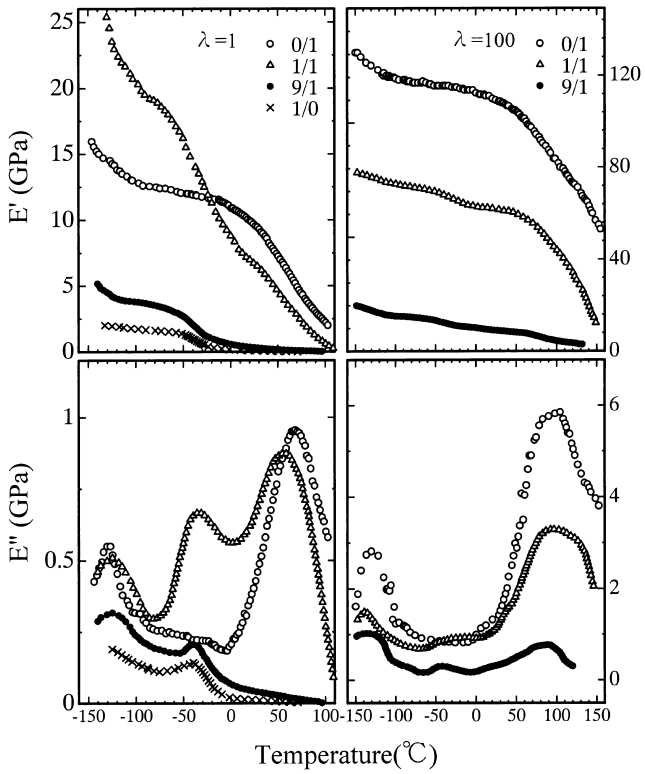

Fig. 11. Temperature dependence of the storage and loss moduli for EDAM-I/UHMWPE blend films and UHMWPE, EDAM-I films at the indicated draw ratios.

much lower than those (68 GPa) of the 1/1. This is obviously due to the fact that the EDAM molecules within the 9/1 compositions take a random orientation, while those within the 1/1 compositions orient predominantly with respect to the stretching direction (see Fig. 5).

The temperature dependence of E'' is sensitive to the introduction of EDAM-I. For the 1/1 compositions, three dispersion peaks, α, β and γ relaxations, are observed. The α relaxation is essentially associated with crystal dispersion. For the blend films, the α relaxation is related to co-crystallites of UHMWPE and EDAM. No α relaxation peak is observed for the 9/1 composite films with $\lambda = 1$ because of a very few amounts of UHMWPE crystallites, and the appearance of the α dispersion with $\lambda = 100$ is due to the growth of crystallization of UHMWPE by elongation. On the other hand, the α relaxation for the 1/1 compositions can be observed for the undrawn films because of large amount of co-crystallites of EDAM and UHMWPE. The increase in the magnitude with elongation is due to an increase in crystallinity by the promotion of co-crystallization of UHMWPE and EDAM chains. The β relaxation appears around -35 °C. Here we must emphasize that the β relaxation cannot be assigned as glassy transition. In accordance with the Arrhenius plots in the previous paper [2], the activation energy of EDAM-I and EDAM-II were 146 and 139 kJ/mol, respectively, which are higher than the values (114–115 kJ/mol) obtained for branched polyethylene (G201 and G808) [2]. Accordingly, it was concluded that together with positron annihilation measurements, the β relaxation of polyethylene is generally associated with large motion of amorphous chains. Judging from a very small peak concerning the β relaxation of undrawn UHMWPE homo-polymer film, the β relaxation is mainly due to the contribution from the large motion of amorphous chains of EDAM. The β relaxation peak magnitude becomes lower with draw ratio λ. But, the peak also can be observed for the 9/1 blend film with $\lambda = 100$. This means that under elongation, the crystallization of ethylene sequences of EDAM is suppressed by DAM side groups, even when the EDAM chains within the 1/1 composite films are oriented predominantly with respect to the stretching direction. Namely, most of the oriented EDAM chains are maintained as amorphous chains with highly ordered arrangement. The γ relaxation, associated with the motion of a short chain segment in the amorphous phase, is observed around -130 °C. This magnitude of the dispersion peak becomes higher with increasing EDAM content because of a decrease in the crystalline phase by introducing EDAM.

To make clear the dispersions of the blend films, positron annihilation is adopted in this paper, since it is well known that an increase in the free volume holes can be clearly estimated by positron annihilation [18]. Actually, the positron annihilation is one of the useful techniques used to investigate the relaxation characteristics of amorphous chains [19–25]. As described in the previous paper [2], positrons emitted from ^{22}Na induce radiation effect on polymer samples and electrons are excited from the constituent atoms. These electrons are trapped in a shallow potential, which are formed at low temperature far below the glass temperature (T_g). The increase in these trapped electrons is observed as the intensity (I_3) of the long-lived component of ortho-positronium (o-Ps) increases.

Fig. 12 shows the variations of o-Ps intensity I_3 and its lifetime τ_3 of the 9/1 composition of EDAM-I/UHMWPE blends with $\lambda = 1$ and 100 as a function of temperature. The variation of I_3 shows 'V' shape with a minimum value at -50 °C. The positron irradiation was done for 30 h at -250 °C. Even so, the trapped electrons do not reach the equilibrium state. Here we shall briefly discuss the reason. For the branched PE (G201), intensity (I_3) attained saturation at 40% after 10 h of measurements, while the intensity (I_3) of EMMA-I with 3.0 mol% polar groups of MMA attained 30% after 120 h of measurements. The lifetime (τ_3), however, shows no obvious change between these two samples. This result can be explained within the framework of the spur model [26,27] of o-Ps formation in terms of the trapping of positrons (and may be electrons) by the polar groups, –C=O, in EMMA [28–30]. In the case of PE, a fast increase in I_3 at -240 °C in comparison with the value for EMMA has been explained in terms of the storage of weakly bound electrons and the high mobility of positrons in PE. Positrons can move out of the terminal spur with a size of about 5–10 nm and diffuse to a distance about 70 nm [31] within the diffusion distance, and

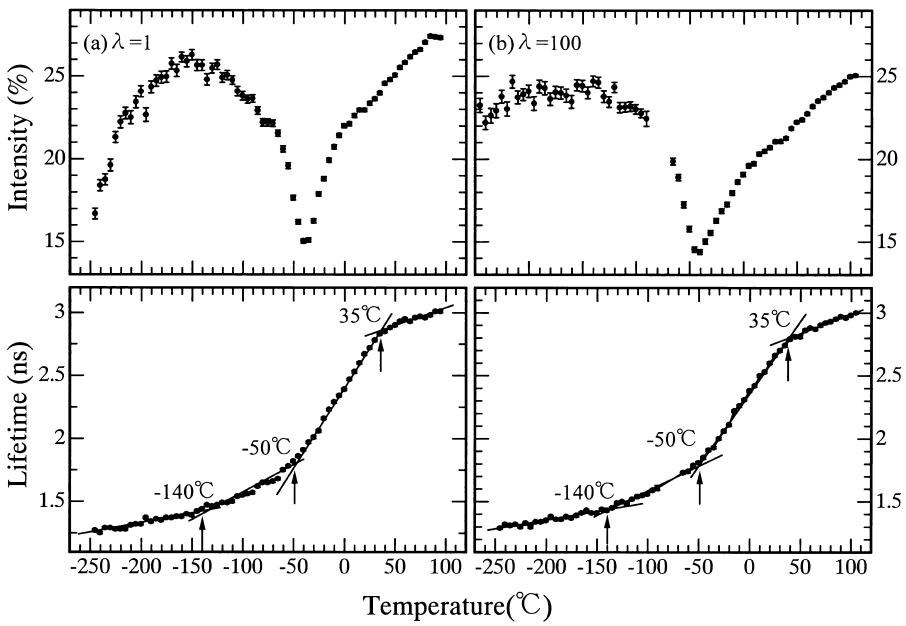

Fig. 12. Intensity (I_3) and lifetime (τ_3) of the long-lived component of the ortho-positronium (o-Ps) as a function of temperature for EDAM-I/UHMWPE = 9/1 composition films at the indicated draw ratio.

positrons can meet trapped electrons. This phenomenon causes an increase of o-Ps formation. However, in the case of EMMA, the positron diffusion length is expected to be shorter due to the trapping of positrons by polar –C=O, and positrons do not have sufficient time to meet weakly bound electrons. The results of Hirade et al. [32] show that the same increase (~12%) of o-Ps formation in EMMA requires nearly 100-times higher concentrations of weakly bound electrons ($\sim 10^{17}\mathrm{cm}^{-3}$), than in the case of PE. Hence, o-Ps formation is limited to within a limited space, and the slow increasing rate of o-Ps formation is related to the necessity of accumulating trapped electrons within the small space [33]. Anyway, we must emphasize that the life time (τ_3) to estimate relaxation modes is almost independent of the saturations of trapped electron at −250 °C.

The secondary electrons escaped from the positron spur could be easily tapped in shallow potentials formed between polymer chains when the motions of the molecular chains and groups are frozen at low temperature. Accordingly, I_3 increases up to −140 °C. Beyond −140 °C, I_3 begins to decrease with increasing temperature and attains to a minimum at about −50 °C. This is due to the fact that activation of molecular chain and group motion could bleach the trapped electrons with increasing temperature [34] and consequently the o-Ps intensity would be greatly reduced. Accordingly, positron annihilation can detect the motion of polymer chains and groups at low temperature by the variation of the o-Ps intensity. In accordance with Suzuki et al. [35], the minimum temperature of I_3 is due to the fact that the local motion causes a large (macro-Brownian) movement of polymer chains in the amorphous phase. Accordingly, most of shallow potentials may be smeared out by the movement; the trapped electrons may then also disappear. If this is the case, the molecular motion at low temperature affects the trapped electrons in a shallow potential, and consequently the variation in I_3 is closely related to the relaxation temperature as a secondary effect.

Beyond −50 °C I_3 increases again. As discussed before [2], this is due to an apparent increase in the number of holes detected by positron annihilation because of the thermal expansion of the holes at elevated temperatures. The very small holes, which cannot be detected by positron annihilation at temperature < −50 °C, can be observed by an increase in the size by thermal expansion.

The lifetime τ_3 is well-known to be related to the hole size by using Tao's equation [16]. The longer is τ_3, the bigger is the hole size in a polymer solid. As shown in Fig. 11, there exist two transitions of τ_3 for the 9/1 composition films −50 °C. The first transition at around −140 °C close to the point that I_3 begins to decrease with increasing temperature. The second transition at −50 °C corresponds to the minimum point of I_3. The third transition at around 35 °C shall be discussed later.

Fig. 13 shows the transitions for the 1/1 composite film with $\lambda = 1$ observed for the blends. Three transitions appeared at around −140, −50 and 30–40 °C, respectively. Comparing the three transitions of τ_3 with the mechanical dispersion peaks in Fig. 12, it turns out that the β relaxation around −35 °C in Fig. 11 corresponds to the second transition and the γ dispersion around −130 °C, the first transition. The good agreement between the transitions of τ_3 estimated by positron annihilation and mechanical dispersions by visco-elastic measurements provides that the established concept of the β and γ dispersions for polyethylene is correct. Namely, the γ dispersion corresponds to the local relaxation mode of polyethylene chains

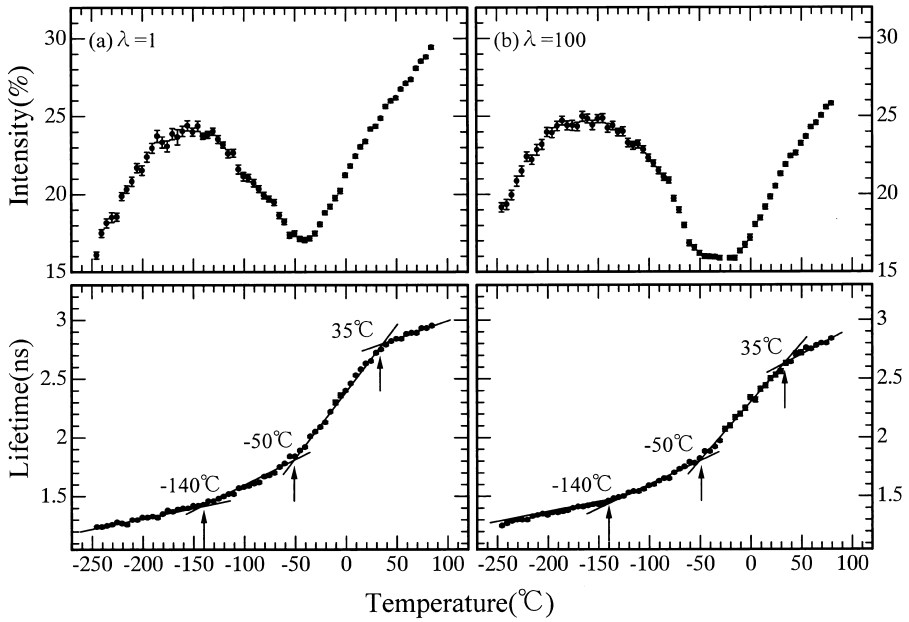

Fig. 13. Intensity (I_3) and lifetime (τ_3) of the long-lived component of the ortho-positronium (o-Ps) as a function of temperature for EDAM-I/UHMWPE = 1/1 composition films at the indicated draw ratio.

and the β dispersion is the contribution from the motion of the amorphous chains. Therefore, positron annihilation is a useful tool to detect some weak motion of polymer groups and chains at low temperature.

The temperature dependence of τ_3 shown in Fig. 13 is quite different from that observed for polyethylene films. Namely, the second transition of τ_3 is observed clearly for the 1/1 composite films with $\lambda = 100$ but not for the corresponding UHMWPE [36]. This is due to the difference of mobility of amorphous chains. Namely, the crystallinity of ultradrawn polyethylene ($\lambda = 100$) was higher than 90%. This justifies that the β relaxation also can not be observed using a dynamic mechanical measurement for ultradrawn polyethylene with $\lambda = 100$ (see Figs. 11 and 12).

The third transition in Figs. 12 and 13 is thought to be due to the partial melting of unstable small crystallites. This phenomenon is thought to be due to a very small peak around 30–40 °C of the DSC curves (see Fig. 8). Such small peak has never been observed for polyethylene homopolymer. This indicates that very small EDAM crystallites are much less stable than UHMWPE crystallites.

Finally, we must emphasize that the same experiments carried out for EDAM-I were also done for EDAM-II. A series of experimental results obtained for the blends of EDAM-II and UHMWPE blends were similar to the results for the blends of EDAM-I and UHMWPE, although the DAM content as side groups of EDAM-II is higher than that of EDAM-I (see Table 1) and the mechanical properties such as stress relaxation and the morphology of EDAM-II observed by Hv light scattering are slightly different from those of EDAM-I. Accordingly, the results for EDAM-I were listed in this paper.

4. Conclusions

EDAM with 3.9% DAM side groups was blended with UHMWPE in solution using decalin as solvent. The dry blend gels had ability to form uniform films and could be elongated to more than 200-fold even for the blend with 90% EDAM content. The ultra-drawing mechanism was investigated by using DSC, WAXD, and SAXS, ^{13}C solid-state NMR and positron annihilation measurements. As the results, it was concluded that the drawing behavior depends on the EDAM contents. Namely, EDAM and UHMWPE chains were crystallized independently for the 9/1 composite films. The greatest drawability for the 9/1 composition films was attributed to only molecular chains of UHMWPE forming large crystal lamellae with highly orientation on the film surface and keeping a suitable number of entanglements ensuring the crystal transition from a folded to a fibrous type. However, most of EDAM chains maintained a random orientation in spite of highly orientation of UHMWPE chains. While ethylene sequences of EDAM chains and UHMWPE chains within the 1/1 compositions were co-crystallized under gelation and drying process and the EDAM chains were also oriented together with UHMWPE chains under elongation process. Such morphological difference caused large difference of the mechanical properties between the 9/1 and 1/1 composite films. For the 1/1 composite films with $\lambda = 100$, the storage modulus E' reached 68 GPa at 20 °C. In contrast, the values of E' of the 9/1 composite films with $\lambda = 100$ are 10 GPa, which was much lower than E' of the 1/1 compositions. This was obviously due to the fact that most of EDAM molecules within the 9/1 composite films take a random orientation, while those within the 1/1 composite films orient drastically

with respect to the stretching direction. The temperature dependence of E'' of the 1/1 composite film was quite different from that of the corresponding UHMWPE homopolymer films. Namely, the β relaxation of the blends could be observed clearly because of low crystallinity of oriented EDAM main chains, while no peak was observed for the corresponding UHMWPE films. This phenomenon was in good agreement with temperature dependence of the intensity (I_3) of the long-lived component of ortho-positronium (o-Ps) and its lifetime τ_3. The detailed analysis of the positron annihilation measurements provided that the first, second and third transitions of τ_3 of the 9/1 and 1/1 composite films correspond to the γ, β, and α relaxations measured by visco-elastic measurements.

References

[1] Ma L, Bin Y, Sakai Y, Chen Q, Kurose H, Matsuo M. Macromolecules 2001;34:4802.
[2] Ma L, Suzuki T, He C, Chen Q, Chen, Kurosu H, Matsuo M. Macromolecules 2003; in press.
[3] Smith P, Lemstra PJ, Pipper JPL, Kiel AM. Colloid Polym Sci 1980; 258:1070.
[4] Kanamoto T, Tsuruta A, Tanaka K, Takeda M, Porter RS. Polym J 1983;15:327.
[5] Kanamoto T, Tsuruta A, Tanaka K, Takeda M, Porter RS. Macromoleciules 1988;21:470.
[6] Matsuo M, Sawatari C. Macromolecules 1986;91:2036.
[7] Ogita T, Yamamoto R, Suzuki N, Ozaki F, Matsuo M. Polymer 1991; 32:822.
[8] Sawatari C, Shimogiri S, Matsuo M. Macromolecules 1987;20:1041.
[9] Sawatari C, Satoh S, Matsuo M. Polymer 1990;32:1456.
[10] Matsuo M, Sawatari C, Ohhata T. Macromolecules 1988;21:1317.
[11] Chen Q, Luo HJ, Yang G, Xu DF. Polymer 1997;38:1203.
[12] Shimizu Y, Harashina Y, Sugiura Y, Matsuo M. Macromolecules 1995;28:6889.
[13] Ando I, Sorita T, Yamanobe T, Komoto T, Sato H, Deguchi K, Imanari M. Polymer 1985;26:1864.
[14] Earl WL, VanderHart DL. Macromolecules 1979;12:762.
[15] VanderHart DL. J Chem Phys 1976;64:830.
[16] Matsuo M, Sawatari C, Nakano T. Polym J 1986;18:759.
[17] Sawatari C, Matsuo M. Macromolecules 1989;22:2968.
[18] Tao SJ. J Phys Chem 1972;56:5499.
[19] Walender M, Maurer FH. J Mater Sci Forum 1992;105:1181.
[20] Suzuki T, Oki Y, Numajiri M, Miura T, Kondo K, Ito Y. Radiat Phys Chem 1995;45:657.
[21] Levey B, Lalovic M, Ache HJ. J Chem Phys 1989;90:3282.
[22] Zhang Z, Ito Y. Radiat Phys Chem 1991;38:221.
[23] Suzuki T, Oshima N, Miura T, Oki Y, Numajiri M. Polymer 1997;37: 5521.
[24] Uedono A, Kawano T, Tanigawa S, Ban M, Kyoto M, Uozumi T. J Polym Sci Part B 1997;35:1601.
[25] van Krevelen DW, Hoftyzer PJ. Properties of polymers. Amsterdam: Elsevier; 1976.
[26] Mogensen OE. Positron annihilation in chemistry. Berlin: Springer; 1995.
[27] Ito Y. J Radianal Nucl Chem 1996;210:327.
[28] Kobayashi Y, Wang CL, Hirata K, Zheng W, Zhang C. Phys Rev B 1998;58(9):5384.
[29] Nagai Y, Hasegawa M, Kobayashi Y, Wang CL, Zheng W, Zhang C. Phys Rev B 1999;60:11863.
[30] Suzuki T, He C, Shantarovich V, Kondo K, Hamada E, Matsuo M, Ma L, Ito Y. Radiat Phys Chem 2003; in press.
[31] Bursa RS, Duarte Naia M, Margoni D, Zecca A. Appl Phys 1995;A60: 447.
[32] Hirrade T, Maurer FH, Eldrup M. Radiat Phys Chem 2000;58:465.
[33] Suzuki T, He C, Kondo K, Hamada E, Matsuo M, Ma L, Ito Y. Radiat Phys Chem 2003; in press.
[34] Chen ZO, Suzuki T, Kondo K, Uedono A, Ito Y. Jpn J Appl Phys 2001;40:5036.
[35] Suzuki T, Kondo K, Hamada E, Ito Y. Radiat Phys Chem 2000;58: 465.
[36] Matsuo M, Ma L, Azuma M, He C, Suzuki T. Macromolecules 2002; 35:3059.